Cancer Chemother Pharmacol (2006) 57: 741–754
DOI 10.1007/s00280-005-0113-5

ORIGINAL ARTICLE

Diane F. Matesic · Kimberly N. Villio · Stacey L. Folse
Erin L. Garcia · Stephen J. Cutler · Horace G. Cutler

Inhibition of cytokinesis and akt phosphorylation by chaetoglobosin K in *ras*-transformed epithelial cells

Received: 1 April 2005 / Accepted: 1 August 2005 / Published online: 28 October 2005

Abstract *Purpose*: Chaetoglobosin K (ChK), a bioactive natural product previously shown to have anti-tumor promoting activity in glial cells and growth inhibitory effects in *ras*-transformed fibroblasts, inhibited anchorage-dependent and anchorage-independent growth in *ras*-transformed liver epithelial cells. The purpose of this study was to identify cellular targets of ChK that mediate its anti-tumor effects. *Methods:* Anchorage-independent cell growth assays, using soft agar-coated dishes, and anchorage-dependent growth assays were performed on transformed WB- *ras*1 cells. Phase/contrast and fluorescent microscopy were used to visualize cell morphological changes and DAPI-stained nuclei. Analyses of p21 Ras membrane versus cytosolic forms, p44/42 mitogen-activated protein kinase (MAPK) phosphorylation, Akt kinase phosphorylation and connexin 43 phosphorylation were performed by Western blotting. Gap junction-mediated cellular communication was measured by fluorescent dye transfer. *Results*: Treatment of WB- *ras*1 cells with a non-cytotoxic dose of ChK inhibited both anchorage-dependent and anchorage-independent growth. Inhibited cells were generally larger and less spindle-shaped in morphology than vehicle-treated cells, many of which were multinucleate. Removal of ChK induced cytokinesis and a return to predominantly single-nucleate cells, suggesting that ChK inhibits cytokinesis. The proportion of membrane-associated versus cytosolic forms of p21 Ras was unchanged by ChK treatment, suggesting that ChK does not act as a farnesylation inhibitor. ChK treatment decreased the level of phosphorylation of Akt kinase, a key signal transducer of the Phosphatidylinositol 3-kinase pathway. In contrast, ChK had no effect on phosphorylation of p44/42 MAPK, which mediates the MAPK/ERK Ras effector pathway. Phosphorylation of the gap junction protein, connexin 43, shown previously to increase following treatment with other anti-Ras compounds, was also not altered by ChK, which correlated with its lack of effect on gap junction-mediated cellular communication. *Conclusions*: Our results demonstrate that ChK inhibits Akt kinase phosphorylation and cytokinesis in *ras*-transformed cells, which likely contribute to its ability to inhibit tumorigenic growth.

Keywords Cytokinesis · Oncogene · Akt kinase · Multinucleate

Abbreviations ANOVA: Analysis of variance · BSA: Bovine serum albumin · ChK: Chaetoglobosin K · Cx43: Connexin 43 · DMSO: Dimethylsulfoxide · EtOH: Ethanol · GSK-3β: Glycogen synthase kinase-3β · MAPK: Mitogen-activated protein kinase · NBT/BCIP: Nitroblue tetrazolium/5-bromo-4-chloro-3-indoyl phosphate · PI-3 kinase: Phosphatidylinositol 3-kinase · PBS: Phosphate-buffered saline · PMSF: Phenylmethylsulfonyl fluoride · PVDF: Polyvinylidene fluoride · SDS: Sodium dodecyl sulfate

Introduction

Normal mammalian Ras proteins mediate cellular proliferation, differentiation, and survival by linking signals from the cell membrane to downstream cytoplasmic or nuclear effectors. Ras proteins are a closely-related group of 21 kD membrane-bound GTP/GDP exchange proteins that are expressed in three forms, H-Ras, K-Ras, and N-Ras [1–3]. The *ras* genes in normal cells are proto-oncogenes that, when mutated, become oncogenes, expressing altered p21 Ras proteins that contribute to the transformed phenotype. *Ras* genes are frequently mutated genes [2], with mutations appearing in at least 30% of human cancers [4]. *Ras* mutations at codons 12,

D. F. Matesic (✉) · K. N. Villio · S. L. Folse · E. L. Garcia
S. J. Cutler · H. G. Cutler
Department of Pharmaceutical Sciences, Mercer University,
3001 Mercer University Drive, Atlanta, GA 30341, USA
E-mail: matesic_df@mercer.edu
Tel.: +678-5476241
Fax: +678-5476423

13, 59, and 61 can result in a constitutively active state in which Ras is not inactivated by GTPase-activating proteins (GAPs) [5], and the GTP-bound "on" state persists. This type of mutation contributes to a tumorigenic phenotype and is seen in a wide variety of neoplastic cells, such as colon, pancreas, and lung carcinoma cells. Ras-induced cellular transformation is mediated by interactions with three major downstream effectors: Raf kinases, which activate MAP kinase signaling pathways [4, 6]; Phosphatidylinositol 3-kinase (PI-3 kinase), which mediates Ras-induced cytoskeletal reorganization [7]; and RalGEFs, which potentiate [8] or induce [4] oncogenic transformation of mammalian cells. *Ras*-transformed cells exhibit phenotypic properties that include anchorage-independent growth, changes in cell morphology, an altered cytoskeleton, and a reduction in gap junction-mediated intercellular communication [1, 7, 9–11]. In both normal and transformed cells, association with the plasma membrane is required for the biological activity of p21 Ras. Farnesylation at the carboxy terminal CAAX motif at cysteine residue 186 of Ras by farnesyltransferase is required for anchorage in the plasma membrane [12–14]. Indeed, farnesylation inhibitors have been shown to disrupt p21 Ras activity in both normal and tumorigenic cells [1, 15, 16]. Because of their pivotal role in growth regulation and cellular transformation, Ras proteins have become key targets for development of drugs to block or reverse their altered function in human cancers [1, 2].

Chaetoglobosin K (ChK), an indolylcytochalasin derived from the phytopathogenic fungus *Diplodia macrospora* [17], has previously been shown to inhibit growth of *ras*-transformed fibroblasts [11] and to prevent tumor promoter-mediated processes [18]. This compound was found to cap the plus-ends of F-actin, which was proposed to contribute to its anti- *ras* oncogenic activity via a PI-3 kinase-mediated pathway [11]. In the present study, we report inhibition of growth by ChK in *ras*-transformed liver epithelial cells, including anchorage-independent growth. ChK treatment promoted formation of multinucleate cells via inhibition of cytokinesis, suggesting that this may be one mechanism for its cytostatic effects. In order to further elucidate the mechanisms involved in the antitumor effects of this compound, we studied its effects on p21 Ras farnesylation, the p44/42 MAPK and PI-3 kinase pathways, and gap junction-mediated cellular communication. The low toxicity of ChK at effective growth-inhibitory concentrations earmarks this compound for further studies on its potential therapeutic use.

Materials and methods

Materials

Alpha modification of Eagle's media, phosphate-buffered saline (PBS), L-glutamine, Trypsin, HEPES, and G418 (selective antibiotic) were purchased from Fisher Scientific (Pittsburgh, PA, USA). Lucifer Yellow-CH, Neutral Red solution, phenylmethylsulfonyl fluoride (PMSF), iodoacetamide, normal goat serum, Ponceau S Red staining solution, protease inhibitor cocktail, and sterile dimethylsulfoxide (DMSO) were purchased from Sigma Chemical Co. (St Louis, MO, USA). Fetal bovine serum (FBS) was purchased from Gibco-BRL (Carlsbad, CA, USA) or Sigma. Connexin 43 (Cx43)-specific monoclonal antibody (MAB3086) was purchased from Chemicon International (Temecula, CA, USA), and fluorescent-conjugated secondary antibodies were purchased from Jackson Immunoresearch Laboratories (West Grove, PA, USA). Biotin-antimouse IgG antibody and alkaline phosphatase-conjugated streptavidin were purchased from ICN Biomedicals, Inc. (Irvine, CA, USA). Phospho-p44/p42 MAPK (Thr202/Tyr204) polyclonal antibodies, p44/42 MAPK polyclonal antibodies, MAPK phosphorylation inhibitor (MEK1/2 inhibitor-U0126), phospho-Akt (ser473 and thr308), Akt, and phospho-GSK-3β (ser9) polyclonal antibodies were purchased from Cell Signaling Technology (Beverly, MA, USA). Aquapolymount was purchased from Polysciences, Inc. (Warrington, PA, USA), and dieldrin was purchased from Accustandard (Bedford, MA, USA). Tris buffer, glycine, sodium dodecyl sulfate (SDS), nonfat dry milk (NDM), DC protein assay kit, alkaline phosphatase color development kit, prestained molecular mass standards, and immunoblotting paper were purchased from Biorad (Hercules, CA, USA). Polyvinylidene difluoride (PVDF) membranes were purchased from Millipore (Bedford, MA, USA) or Biorad.

Methods

Cell cultures

WB- *ras* and WB- *neo* rat liver epithelial cells, derived from WB-F344 cells [10], were subcloned from single colonies. The resulting subcloned cell lines, designated WB- *ras*1 and WB- *neo*3, were used between passages 6 and 20. Cells were grown in α-MEM supplemented with 5% FBS, 2 mM L-glutamine, and 400 mM G418. Cells at 90–100% confluency were subcultured by trypsinization, plated at 5–25% confluency, depending on the experiment, and incubated at 37°C in an atmosphere containing 5% CO_2.

Cell growth assays

Cells were plated at 5–10% confluency onto 35 mm^2 dishes, culture medium (lacking G418) was added to 2 ml, and allowed to attach overnight. Cells were treated with varying concentrations of vehicle (DMSO) or ChK in DMSO and incubated at 37°C for varying times. The DMSO concentration was kept below 1%. Following the desired incubation time, medium was removed and cells were washed twice with PBS.0.2 ml of 0.25% trypsin solution and 0.8 ml of PBS were added until cells

detached from the dish. Medium, 1.0 ml, was then added and cells in suspension were counted as is or after dilution with 2–10 ml of medium, using a hemocytometer to determine the number of cells per dish. Triplicate dishes were counted for each time point except where noted.

For growth in soft agar, 2% agar was mixed with an equal volume of culture medium and 1.5 ml of this mixture was plated onto each well of a 6-well culture dish. Plates were stored overnight or up to 1 week at 4°C. WB- *ras*1 cells were trypsinized and suspended in a medium containing 2% agar and either vehicle (0.1% DMSO) or 1 μM ChK and plated onto the agar base at 5–10,000 cells/well. Colonies were allowed to grow for 1 week. Medium on top of the agar was removed and 1 ml of fresh medium containing vehicle or 1 μM ChK was added. Colonies were allowed to grow for another week. Digital photographs of randomly chosen fields were taken using a Leitz inverted microscope equipped with a 10X objective lens. Colonies were counted and diameters were measured using Image Tool 3.0 software (UTHSCSA, San Antonio, USA).

Protein concentration assay

Protein concentrations were determined using the Bio-rad DC protein assay. BSA was used as a standard and absorbances were read at 750 nm using a Biotek or Tecan plate reader.

Trypan blue staining

Cells were plated onto 35 mm^2 dishes at 10–15% confluency and treated with varying concentrations of 0, 0.5, 1, or 2 μM ChK in DMSO for 24 h or 1 μM ChK for 2–5 days. Cells were washed with PBS and incubated with 0.25% trypsin in PBS to detach cells, followed by addition of an equal volume of 0.4% Trypan blue [19] and incubated for 4 min. Unstained (viable) and blue-stained (non-viable) cells were counted using a hemocytometer. At least three separate dishes were counted for each ChK concentration or time point, and each dish was counted twice. The average of the two values was used as one determination. As a positive control for cytotoxicity, three separate vehicle-treated dishes were treated with 0.1% sodium azide, 1.5% methanol, and 0.5% acetic acid for 1 h.

Dye transfer assay of gap junction-mediated cellular communication

Cells grown in 35 mm^2 dishes were washed once with PBS containing 0.5 mm $CaCl_2$ and 0.5 mm $mgCl_2$ and twice with PBS. One milliliter of 0.5 mg/ml Lucifer Yellow in PBS was added and several areas of the cell monolayer were scored with a surgical blade to allow entry of Lucifer Yellow. After 90 s, the dye was removed and cells were washed once with Ca^{2+}/Mg^{2+} PBS followed by two washings with PBS. Cells were then fixed with 4% formaldehyde in PBS. Fluorescence was observed using a Leitz inverted microscope equipped with a 10× objective lens. Several areas of each test plate were digitally photographed and the number of fluorescent cells in a defined area along the score line was counted. Since cells along the score line were fluorescent, regardless of their ability to communicate, the average number of cells in fully inhibited (dieldrin-treated) samples was subtracted from the total number of cells counted in the various treatment groups to give a better estimate of the number of communication-positive cells. Statistical analyses were performed using Microsoft Excel.

Immunoblot analysis of connexin 43

Membrane-enriched protein fractions were extracted from RG-2 cells grown in 75 cm^2 flasks by lysis in extraction buffer (0.375 ml of 10 mM Tris [pH 7.5], 10 mM iodoacetamide, and 1 mM PMSF) as previously described [20]. Samples were alkalinized by addition of 0.55 ml NaOH, chilled on ice, and sonicated for two 15 s pulses on a Bronson sonicator at 35% maximal power using a microtip. Samples were centrifuged for 30 min a microfuge (14,000 rpm), membrane-enriched pellets were washed with 10 mM Tris (pH 7.5) and 1 mM PMSF (Tris/PMSF buffer) and resuspended in the Tris/PMSF buffer by sonication. Aliquots were removed for protein assay and the remainder solubilized in Laemmli sample buffer [21]. Following electrophoresis on 1 mm thick, 12.5% acrylamide minigels, proteins were transferred to PVDF membranes in transfer buffer containing 0.02% SDS overnight at 20 V. Membranes were washed with deionized H_2O, stained with Ponceau S staining solution for 2–3 min, washed with deionized H_2O, then blocked for 1–2 h at room temperature in block buffer [40 mM Tris (pH 7.5), 4% NDM, 0.1% Tween-20], then incubated in block buffer containing connexin 43-specific antibodies diluted 1:3,000 for 12–24 h at 4°C on a shaker. Membranes were washed in block buffer, incubated for 1–2 h with biotinylated antimouse antibodies diluted 1:400 in block buffer, washed, then incubated for 1 h with streptavidin-conjugated alkaline phosphatase. After washing, immunopositive bands were visualized using the NBT/BCIP detection system.

Immunoblot analysis of p21 ras

Cells were grown to 80–90% confluency in 25 cm^2 flasks, washed with 10 ml of PBS, and extracted with 250 μl of 2% SDS and 1 mM PMSF, and 1:100 dilution of protease inhibitor mix. Lysed cells were scraped, suspensions were transferred to microcentrifuge tubes, and samples were sonicated for two 15 s pulses at room temperature. At one-fourth the final sample volume, 4x Laemmli sample buffer was added. Equal amounts of

protein per lane were separated on 15% acrylamide SDS gels and transferred to PVDF membranes overnight at 20 V. Pan-Ras monoclonal primary antibody, biotin-linked secondary antibody, and streptavidin-conjugated alkaline phosphatase with BCIP/NBT substrates were used to detect p21 Ras bands.

Immunoblot analysis of p44/42 MAPK and phospho-p44/42 MAPK

Cells were grown to 80–90% confluency in 25 cm^2 flasks with or without (vehicle only) treatment with 1 or 2 μM ChK for varying times and washed with 10 ml of PBS. Cells were lysed and proteins solubilized with 250 μl of 2% SDS and 1 mM PMSF, and 1:100 dilution of protease inhibitor mix. Lysed cells were scraped, suspensions were transferred to microcentrifuge tubes, and samples were sonicated for two, 15 s pulses at room temperature. Protein concentrations were determined by Biorad DC assay. To equal amounts of protein/lane at one-fourth the final sample volume, 4x Laemmli sample buffer was added. Proteins were separated on 12.0% acrylamide SDS gels and transferred to PVDF membranes overnight at 20 V or 1 h at 180 V. Membranes were washed with deionized H_2O, stained with Ponceau S staining solution for 2–3 min, washed again with deionized H_2O, scanned, and then blocked using block buffer for 1–2 h. p44/42 MAPK or phospho-p44/42 MAPK polyclonal antibodies diluted 1:2,000 were incubated separately with each of two identical blots in block buffer for 2 h on a shaker at room temperature. Immunopositive bands were detected using alkaline phosphatase conjugated antirabbit secondary antibody with BCIP/NBT as substrates.

Immunoblot analysis of Akt and GSK-3β phosphorylation

Cells were grown to 80–90% confluency in 25 cm^2 flasks with or without (vehicle only) treatment with 1 or 2 μM ChK for varying times, and washed with 10 ml of PBS. Cells were lysed, proteins were solubilized, and samples were sonicated and centrifuged as described above for analysis of p44/42 MAPK phosphorylation. To equal amounts of protein/lane at one-fourth the final sample volume, 4× Laemmli sample buffer was added. Proteins were separated on 12.0% polyacrylamide SDS gels and transferred to PVDF membranes overnight at 20 V or for 1 h at 180 V. Membranes were washed with deionized H_2O, stained with Ponceau S staining solution for 2–3 min, washed again with deionized H_2O, scanned, then blocked using block buffer for 1–2 h. Akt or phospho-Akt (ser473 or thr308-specific) polyclonal antibodies diluted 1:1,000 were incubated separately with each of two identical blots in block buffer for 2 h on a shaker at room temperature. For phospho-GSK-3β detection, phospho-GSK-3β(ser9-specific) polyclonal antibodies were used at 1:1,000 dilution and processed the same as phospho-Akt and Akt blots. Immunopositive bands were detected using alkaline phosphatase conjugated antirabbit secondary antibody with BCIP/NBT as substrates. For densitometric quantification, developed blots were scanned on a HPscanjet 4400C scanner and band intensities measured using UN-SCAN-IT software (version 5.1) from Silk Scientific, Inc. (Orem, UT, USA).

Quantification of multinucleate cells

Cells were plated at 10–15% confluency on 35 mm^2 dishes, treated with 1 μM ChK or vehicle, and allowed to grow for 48 h. Photographs were taken of several areas on each dish. The total number of cells, number of cells with a single nucleus, and number of cells with multiple nuclei were counted in a defined area. In some experiments, cell nuclei were stained with DAPI before microscopic analysis. For reversibility experiments, cells were treated with ChK for 48 h, ChK was then removed by replacing media with media lacking ChK and cells were observed for 24–120 h.

Time-elapsed photomicrography after removal of ChK

WB- *ras*1 and WB- *neo*3 cells plated at low density (1–2% confluency) and treated for 48 h with 1 μM ChK were digitally photographed on a Leitz inverted microscope using a 10x objective lens, and specific areas were marked on the lower surface of the culture dish. Following the removal of media containing ChK, a gentle 2 ml wash with media, and replacement with 2 ml of fresh media, cells were digitally photographed in marked areas at varying time intervals from 1 h to 96 h in order to monitor specific multinucleate cells.

Results

Chaetoglobosin K inhibits growth of *ras*-transformed epithelial cells in culture

Figure 1a shows growth in tissue culture dishes of WB-*ras*1 cells in the presence and absence of 1 μM ChK. Treatment with ChK produced significant inhibition of cell growth as measured by a decrease in the number of cells at 6 days post-treatment compared to vehicle-treated cells. A small but insignificant degree of inhibition was also seen at 2 days post-treatment. Figure 1b shows the concentration-dependent effect of ChK on growth of WB- *ras*1 cells. Based on these data, the IC_{50} for inhibition of growth is estimated to be 0.8 μM ChK.

As shown in Fig. 1c, 1 μM ChK also inhibited the growth of WB- *neo*3 cells in culture dishes. The degree of inhibition at 6 days treatment with 1 μM ChK versus a 6 day vehicle-treatment was lower for WB- *neo*3 cells (40% inhibition) than for WB- *ras*1 cells (88% inhibi-

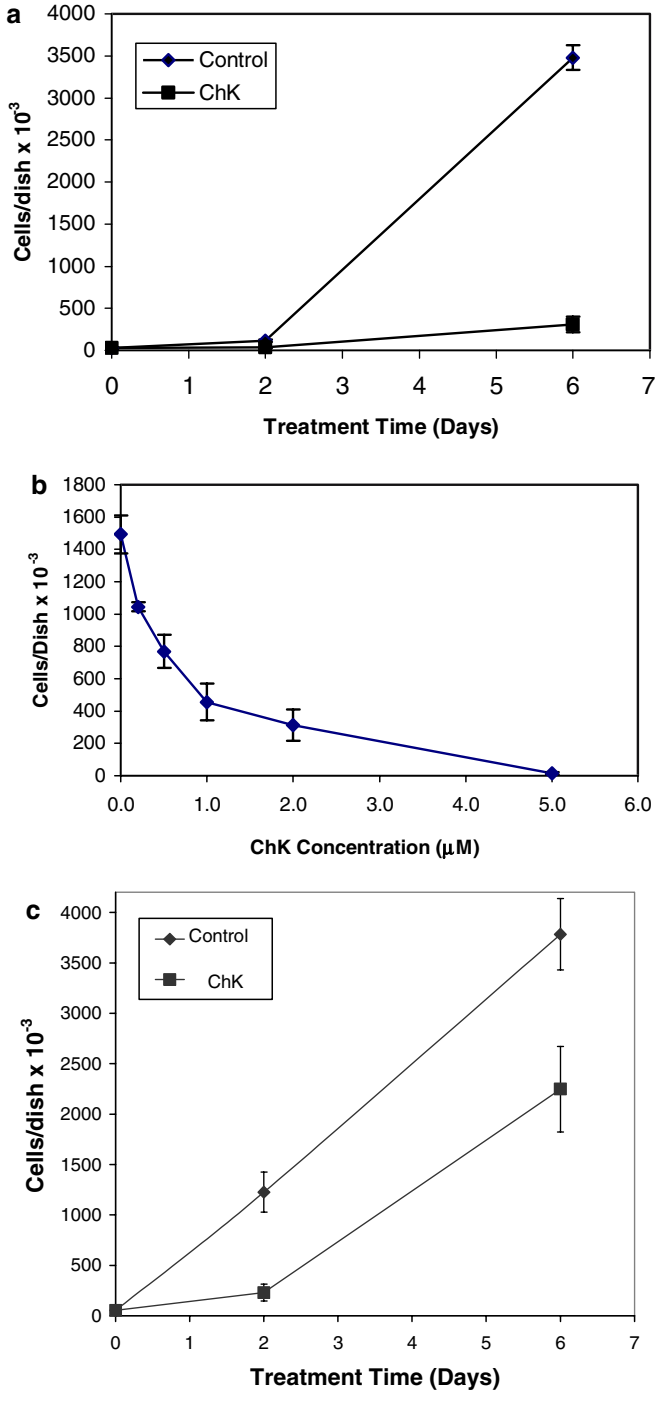

Fig. 1 Effect of ChK on WB- *ras*1 anchorage-dependent cell growth. **a** WB- *ras*1 cells were grown on 35 mm^2 culture dishes to 90–100% confluency over 6 days in the presence or absence of 1 μM ChK. Cells were counted on a hemocytometer on days 0, 2, and 6. Vehicle treated (*filled diamond*); ChK-treated day 0 (*filled square*); data are presented as the mean ± S.D. ($n = 3$) and are representative of two independent experiments; **b** Concentration dependence of the effect of ChK on cell growth. Cells were treated with ChK or vehicle (DMSO) for 4 days at the indicated concentrations. Data are presented as the mean ± S.D. ($n = 3$ or 4 at each concentration). **c** Effect of ChK on WB- *neo*3 cell growth. WB- *neo*3 cells were grown to 90–100% confluence over 4 days in the presence or absence of 1 μM ChK. Cells were counted on a hemocytometer on days 0, 2, and 6. Data are presented as the mean ± S.D. ($n = 3$)

tion). After 6 days of incubation with 1 μM ChK, both WB- *ras*1 and WB- *neo*3 cells increased in number compared to day 1, suggesting that some cell division occurred. When checked for cell viability using Trypan blue staining, 97.6 ± 1.2% of WB- *ras*1 cells and 93.8 ± 5.4% of WB- *neo*3 cells excluded Trypan blue after treatment with 1 μM ChK for 24 h, compared to 96.9 ± 1.0% in vehicle-treated WB- *ras*1 cells and 98.1 ± 1.3% for vehicle-treated WB- *neo*3 cells, suggesting that ChK was not cytotoxic to cells at this concentration. No significant reduction in cell viability was observed by 2 μM ChK treatment of WB- *ras*1 cells for 24 h compared to untreated controls, whereas 10 μM ChK reduced WB- *ras*1 viability to 68.2 + 0.2% ($n = 3$ determinations for each treatment).

Chaetoglobosin K inhibits anchorage-independent growth in soft agar

ChK also inhibited growth of WB- *ras*1 cells in soft agar (Fig. 2b) compared to vehicle-treated control WB- *ras*1 cells (Fig. 2a). Figure 2c shows quantification of soft-agar growth inhibition over 14 days by ChK in WB- *ras*1 cells. The percentage of colonies that were greater than 25 μm in size was lower in the presence of 1 μM ChK (~48%) compared to vehicle-treated controls (~85%). The percentage of colonies greater than 50 μm in size was also lower in ChK-treated cells (~3%) compared to untreated cells (~40%). In contrast, the percentage of colonies less than 25 μm in size was higher in the ChK-treated cells (> 50%) compared to vehicle-treated cells (~15%). Thus, the mean size of the colonies was smaller in ChK-treated cells compared to vehicle-treated cells.

Chaetoglobosin K treatment induces multinucleate cells

Treatment of WB- *ras*1 cells with 1 μM ChK for 48 h resulted in the appearance of cells with multiple nuclei (Fig. 3, panel b, arrows). ChK-treated cells also appeared larger and less spindle-shaped (panel b) than vehicle-treated cells (panel a). Table 1 shows quantification of the number of single versus multiple (2–5) nuclei following treatment with 1 μM ChK for 48 h. In five randomly chosen areas of ChK-treated cells grown in culture dishes, the percentage of cells with multiple nuclei was 77.5 versus 9.2 in control (vehicle-treated) cells. In control cells, multi-nucleate cells never had more than 2 nuclei, whereas ChK-treated multi-nucleate cells had two to five nuclei. Multi-nucleate cells were also present in WB- *ras*1 cells after 24 h treatment with 1 μM ChK or with 24–48 h treatment with 2.5 μM ChK (data not shown). In addition, multi-nucleate cells were detectable in WB- *neo*3 cultures treated with 1 μM ChK for 48 h (Fig. 4, panel c). DAPI staining showed that nuclei in multi-nucleate WB- *ras*1 or WB- *neo*3 cells (Fig. 4 panels d and h) were not noticeably different in size, shape, or staining intensity than nuclei in single-

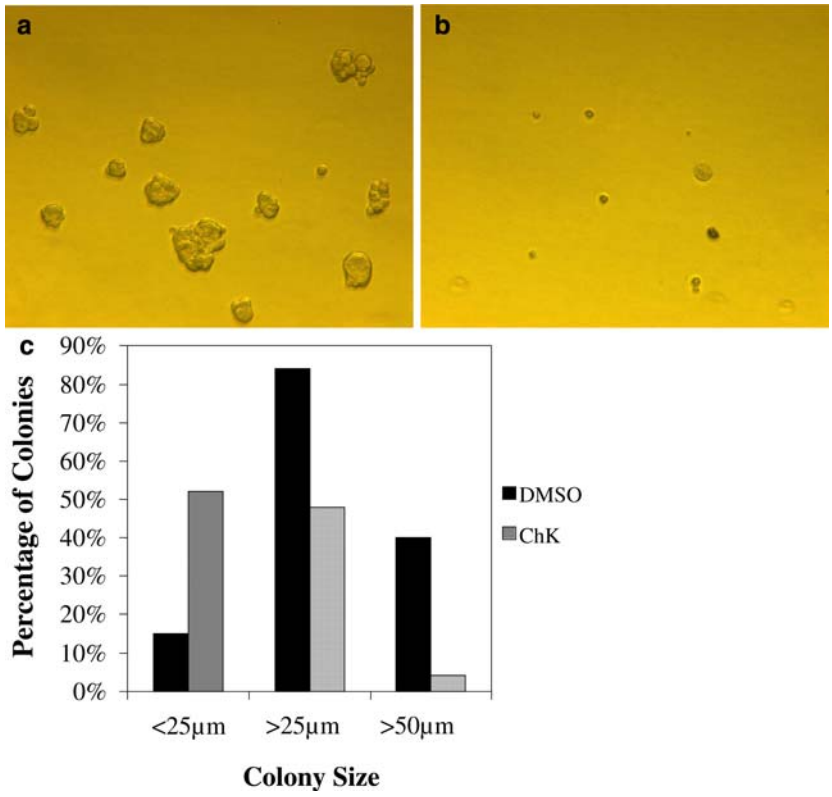

Fig. 2 Effect of ChK onWB-*ras*1 anchorage-independent growth in soft agar. Representative image of cells grown **a** in the presence of vehicle (0.1% DMSO), or **b** 1 µM ChK, for 14 days. The number and size of cell colonies were quantified on day 14 **c**. Data presented are the percentages of colonies in each size category for ChK-treated ($n = 24$) and vehicle-treated control ($n = 33$) wells, and are representative of 2 independent experiments

nucleated cells (Fig. 4, panels b and f). To determine the fate of multi-nucleate cells, ChK was removed following a 48 h treatment with 1 µM ChK and the cells observed at varying time points after removal of ChK. Colonies in which nearly all of the cells had multiple nuclei became predominantly single- nucleate after removal of ChK for 48 h (data not shown). In addition, time-elapsed photomicrography of individual multi-nucleated WB- *ras*1 cells showed that, upon removal of ChK, the cells appeared to undergo cytokinesis into daughter cells with fewer nuclei (Fig. 5, 0–48 h), supporting the idea that ChK inhibits cytokinesis.

Chaetoglobosin K does not alter the relative amount of membrane versus cytosolic forms of p21 Ras

To determine whether ChK inhibited growth by altering the ability of p21 Ras to associate with membranes, cells were treated with 1 µM ChK for 4 h, 1 day, 3 days, or 5 days, hypotonically disrupted in the presence of 2% SDS and protease inhibitors, sonicated, and the resulting total protein extract analyzed by electrophoresis/Western blotting as described in "Methods". P21 Ras has previously been shown [22] to separate into two bands on SDS/polyacrylamide gels; the faster migrating band has been identified as the post-translationally modified farneslyated membrane-attached (m) species and the slower migrating band, the unmodified cytosolic-soluble (s) species. Figure 6a shows no change in the relative amount of the slower migrating band compared to the faster migrating band in 1 or 2 µM ChK-treated cells at 4 h (lanes 8 and 9), 1 day (lanes 10 and 11), or 3 days (lanes 4 and 5). A similar lack of effect on p21 Ras forms was seen in cells treated for 5 days with 1 or 2 µM ChK (not shown). In contrast, treatment of WB- *ras*1 cells with lovastatin, a known farnesylation inhibitor that increases the relative amount of the cytosolic p21 species, caused an increase in the relative amount of the slower migrating band (lanes 6 and 12), as previously reported [23]. These results indicate that ChK does not alter the proportion of membrane versus cytosolic forms of p21 Ras, or the total amount of p21 Ras, in WB- *ras*1 cells at 4 h to 5 day treatment times.

Chaetoglobosin K decreases Akt phosphorylation in WB- *ras*1 cells

Treatment of cells for 24 h with 1 and 2 µM ChK reduced the level of Akt phosphorylation in WB- *ras*1 cells (Fig. 7a, phospho-Akt (ser473), top panel, lanes 4 and 5, compared to vehicle-treated cells, lanes 2 and 3). Total Akt levels were similar in treated (second panel from top, lanes 4 and 5) and untreated cells (lanes 2 and 3). Densitometric scans of the blots indicated that band density in the top panel, lane 4 (2 µM ChK), was 63% and band density in the top panel, lane 5 (1 µM ChK), was 71% of the band density of top panel control lane 2 (after normalization to total Akt levels). A decrease in Akt phosphorylation (ser473) was seen as early as 4 h after treatment with 2 and 5 µM ChK (Fig. 7b, lanes 5–8). Densitometric scans indicated that the average band density of lanes 5 and 6 was 82% and the average band

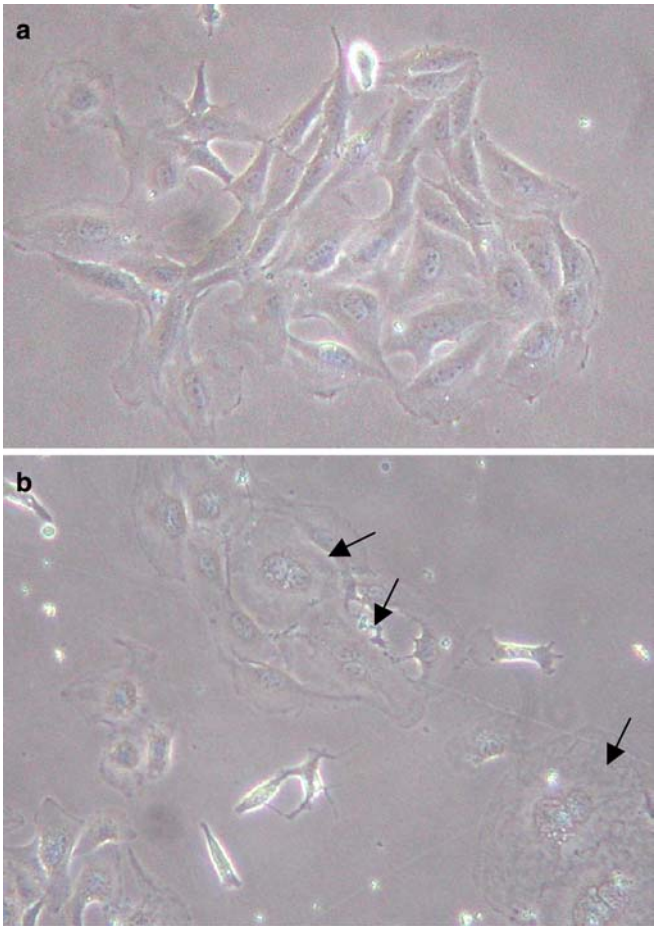

Fig. 3 Effect of ChK on WB- *ras*1 morphology. WB- *ras*1 cells were treated for 48 h **a** in the presence of vehicle (0.1%DMSO) or **b** 1 μM ChK and digital photomicrographs taken using an Olympus inverted phase/contrast microscope and a 20X objective lens. *Arrows point* to cells with multiple nuclei

density of lanes 7 and 8 was 68% of the average band density of control lanes 2–4 (after normalization to total Akt levels). Levels of phospho-Akt in 5 μM ChK-treated cells in this experiment were similar to levels seen in WB-*neo*3 cells (Fig. 7b, lane 9). Decreases in phospho-Akt (ser473) levels were also seen in cells treated with 2 μM ChK for 48 and 72 h (data not shown). In contrast to its effects in WB- *ras*1 cells, Fig. 7c shows that 5 μM ChK had no effect on serine 473 Akt phosphorylation in WB-*neo*3 cells treated for 4 or 24 h (lanes 2–8). However, in addition to its effects on phosphorylation of Akt on serine 473 in WB- *ras*1 cells, ChK also decreased levels of phosphorylation of Akt on threonine 308 (Fig. 7d). Lanes 6 and 7 of Fig. 7d show reduced levels of phospho-Akt (thr308) in cells treated for 48 h with 2 μM ChK, compared to vehicle-treated control cells (lanes 2 and 3). Reduced phosphorylation of Akt on threonine 308 was also seen in cells treated for 24 h with 2 μM ChK (data not shown). To determine whether ChK modulates phosphorylation of a key effector protein of Akt, GSK-3β, Western blot analysis of phospho-GSK-3β(ser9) was performed. Figure 7e shows that ChK reduced phospho-GSK-3β levels in WB- *ras*1 cells treated for 48 h with 2 μM ChK (lanes 4 and 5) compared to vehicle-treated control cells (lanes 2 and 3). Densitometric scans indicated that the average density of the doublet bands in lanes 4 and 5 was 72% of the average density of the doublet bands in control lanes 2 and 3.

Table 1 WB- *ras*1 cells were treated for 48 h with 1 μM ChK or vehicle, and several areas of two separate culture dishes for each treatment digitally photographed

	Control (DMSO)	ChK (1 μM)
Number of cells with a single nucleus	416	57
Number of cells with 2–5 nuclei	42	197
Total number of cells	458	254
Cells with multiple nuclei (%)	9.20	77.50

All cells in selected areas were counted and the total number of cells, number of cells with a single nucleus and number of cells with multiple nuclei counted as indicated

Chaetoglobosin K does not alter p44/42 MAPK phosphorylation in WB- *ras*1 cells

Phosphorylation of p44/42 MAPK was monitored following treatment of WB- *ras*1 cells with 1 or 2 μM ChK for 4 h, 24 h, 48 h, or 5 days. Western blot analysis was performed using antibodies specific for phosphorylated p44/42 MAPK and compared with blots using antibodies that reacted with total p44/42 MAPK protein. Figure 8 shows that ChK had no detectable effect on the degree of MAPK phosphorylation at 4 h (lanes 4 and 5 compared to control lane 2) and 24 h (lanes 6 and 7 compared to control lane 3) treatment. A 48 h or 5 day treatment with 1 or 2 μM ChK also had no detectable effect on the degree of MAPK phosphorylation in WB-*ras*1 cells (data not shown). However, the amount of phosphorylated MAPK was decreased in cells treated for 24 h with a known MAPK phosphorylation inhibitor (lanes 8 and 9 compared to control lane 3).

Chaetoglobosin K does not alter gap junction-mediated communication or connexin phosphorylation

Gap junction-mediated communication is decreased in most tumor cells relative to non-transformed cells of the same origin, including *ras*-transformed epithelial cells [24]. A number of growth-inhibitory antitumor compounds have been shown to upregulate gap junction-mediated communication in *ras*-transformed cells [25, 26]. We performed fluorescent dye-transfer experiments to determine whether ChK had a similar up-regulatory effect on gap junction-mediated communication. Treatment of WB- *ras*1 cells with 1 or 2 μM ChK for 1 h, 6 h, 24 h, and 6 days had no significant effect on gap junction-mediated communication compared to vehicle-treated WB- *ras*1 cells (Fig. 9, graphs in top panels). The

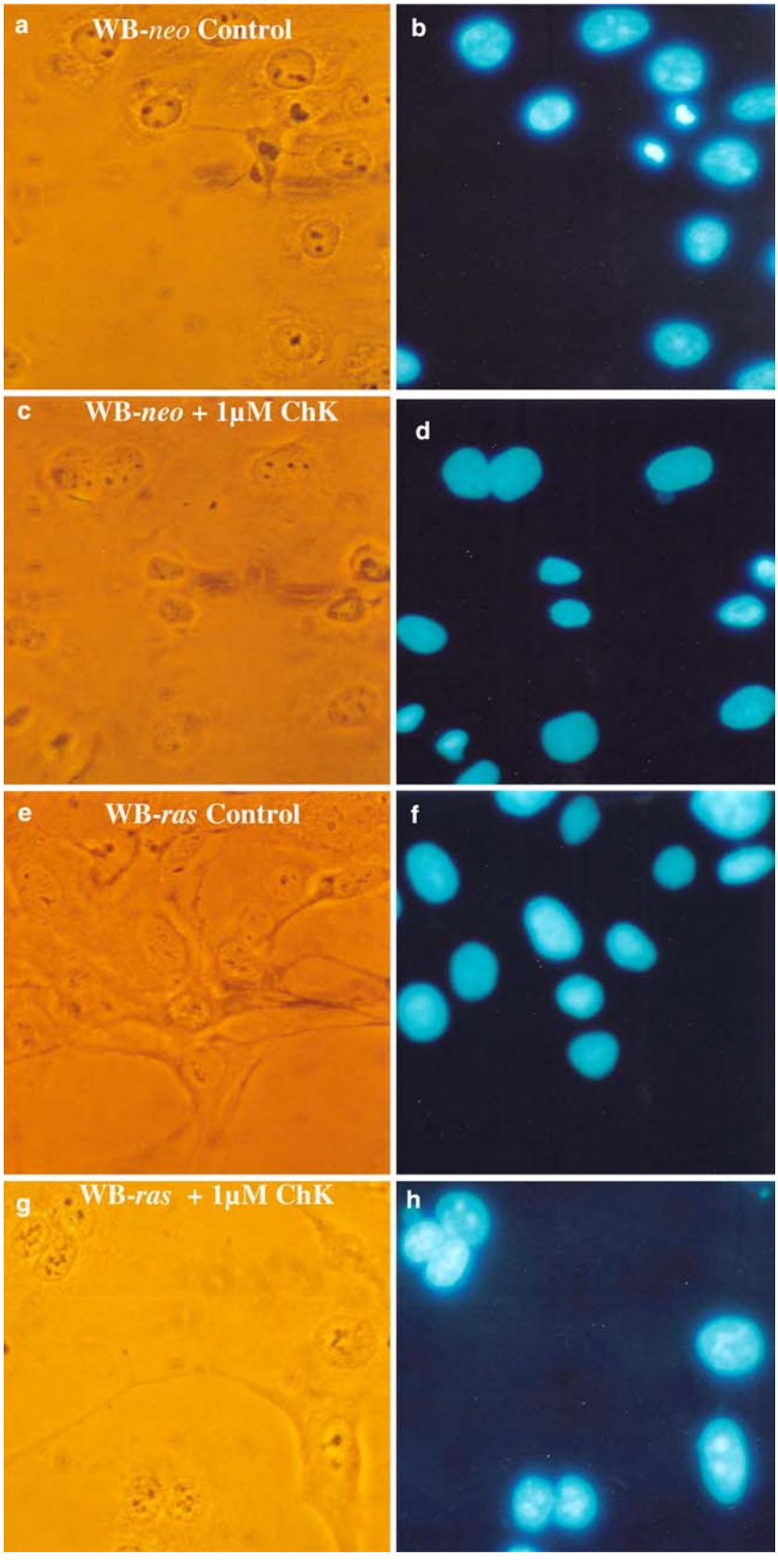

Fig. 4 DAPI staining of WB-*ras*1 and WB- *neo*3 cells. Cells were treated for 72 h with 0.1% DMSO (**a, b, e, f**) or 1 μM ChK (**c, d, g, h**), fixed with 95% EtOH/5% HoAc, and stained with DAPI as described in "Methods." Fluorescent or phase/contrast micrographs were taken using a Leitz Orthoplan microscope and a 40× objective lens

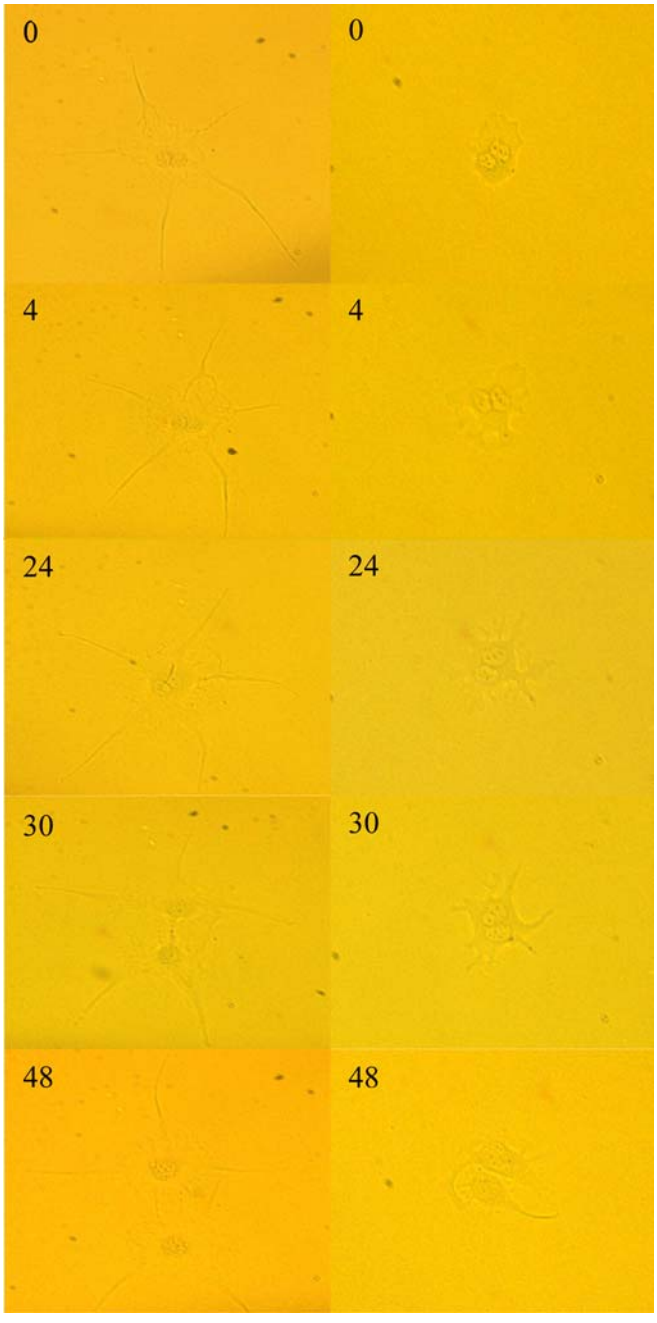

Fig. 5 Induction of cytokinesis by removal of ChK. WB- *ras*1 cells treated for 48 h with 1 μM ChK were washed once with media, then incubated in fresh media containing no ChK for the indicated time periods (hours). Digital photomicrographs were taken from a Leitz Fluorovert microscope using a 25× objective lens. The two *columns* show time-dependent morphological changes of two different cells with multiple nuclei

effect of ChK on communication between WB- *neo*3 cells was not evaluated due to their high basal level of communication.

To determine whether ChK altered the degree of phosphorylation of the gap junction protein, connexin 43, an indicator of its functional state, Western blot analysis of connexin 43 in WB- *ras*1 cells was performed. Figure 9 (bottom panels) shows that vehicle-treated WB- *ras*1 cells primarily expressed the P_0 unphosphorylated band with little to no expression of the phosphorylated P_1 or P_2 (Fig. 9, bottom panels, lanes 2 and 7). WB- *neo*3 cells, in contrast, expressed the P_0, P_1, and P_2 bands (Fig. 9, bottom panels, lane 6), as previously reported [24]. A 1 h, 6 h, or 6 day treatment of WB- *ras*1 cells with 1 or 2 μM ChK did not substantially alter the degree of phosphorylation of connexin 43, compared to vehicle-treated control cells (Fig. 9, bottom panels, lanes 2–5, left and 1–3, right).

Discussion

Our results demonstrate that a single treatment with ChK at a non-cytotoxic concentration produced significant inhibition of anchorage-dependent WB- *ras*1 cell growth by day 6. The small increase in cell number during treatment with ChK suggests that, although cells were dividing at a slower rate than untreated cells, they were still sufficiently viable to undergo cell division. The concentration-dependence analysis yielded a concentration for one-half maximal inhibition of WB- *ras*1 growth of approximately 0.8 μM. These results are consistent with the previously published results by Tikoo et al. [11] that demonstrated growth inhibition of *ras*-transformed fibroblasts at micromolar concentrations. In these studies, ChK was found to induce apoptosis. However, blockage of apoptosis using the inhibitor N1445 [11] failed to block the ability of ChK to inhibit growth of *ras*-transformed fibroblasts, suggesting that induction of apoptosis is not the predominant mechanism for growth inhibition by ChK. In our *ras*-transformed cells, we demonstrate that a non-cytotoxic dose of ChK inhibited growth. While ChK may have induced a low level of apoptosis in our cells, it was not enough to cause significant loss of cell viability in the Trypan blue exclusion assay, compared to vehicle-treated cells. We observed increased numbers of nuclei per cell in ChK-treated WB-*ras*1 cells, suggesting that one anti-proliferative mechanism of ChK may be the inhibition of cytokinesis. Tikoo et al. [11] reported that ChK inhibited actin polymerization via plus-end capping. Since cytokinesis requires mobilization of actin filaments, it would be expected that cells exposed to ChK display decreased cytokinesis, resulting in cells with multiple nuclei. This explains the ability of ChK to induce multiple nuclei and inhibit growth in non-transformed WB- *neo*3 cells. Na et al. [27] observed a similar increase in the number of nuclei per cell in *ras*-transformed WB cells treated with the antitumor compound ET-18-O-CH_3. These authors also proposed inhibition of cytokinesis to explain the observed formation of multinucleate cells. In addition, clonogenic assays suggested that their multinucleate cells had lost colony-forming ability and might be terminally differentiated. In our present study, upon removal of the ChK, most of the multinucleate WB- *ras*1 cells were observed to resume cytokinesis and become predomi-

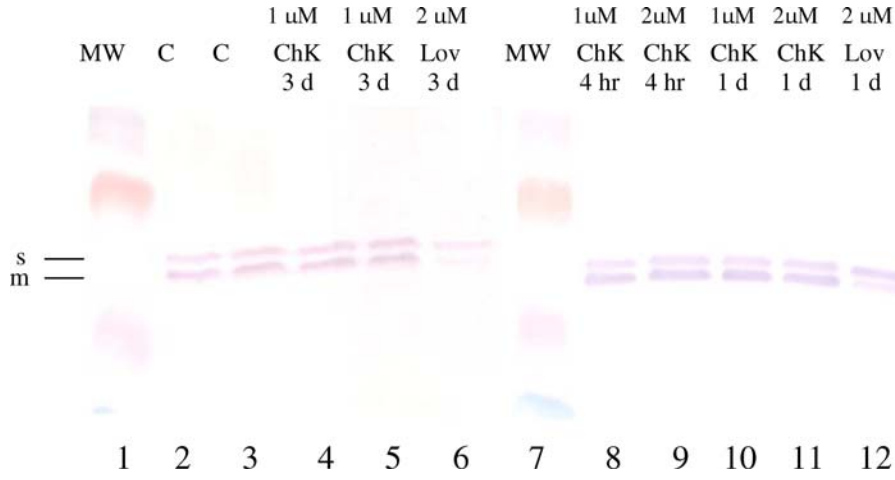

Fig. 6 Effect of ChK on p21 Ras. WB- *ras*1 cells were grown in 25 cm^2 flasks to 90–95% confluency, treated with vehicle or 1 or 2 μM ChK for varying times as indicated and proteins extracted for Western blot analysis of soluble(s) or membrane-associated (m) p21 Ras using a pan-Ras monoclonal antibody as described in "Methods." Treatment groups were: molecular weight markers (*lane 1*); vehicle for 3 days (*lanes 2 and 3, duplicates*); 1 μM ChK for 3 days (*lanes 4 and 5, duplicates*), 4 h (*lane 8*) or 1 day (*lane 10*); 2 μM ChK for 4 h (*lane 9*) or 1 day (*lane 11*); 2 μM lovastatin for 3 days (*lane 6*) or 1 day (*lane 12*). Results are representative of at least two independent experiments

nantly single-nucleate cells. This suggests that the cytostatic effect of ChK is reversible, rather than permanent. Thus, while these two antiproliferative compounds inhibit cytokinesis, they may work through different cellular mechanisms. This is supported by the observation that ET-18-O-CH_3 reduced phosphorylation levels of ERK1/2 (p44/42 MAPK), while ChK did not, as discussed further below.

Although ChK inhibited the growth of the non-tumorigenic WB- *neo*3 cells, it was equally non-cytotoxic to these cells and upon removal of ChK, the WB- *neo*3 cells appeared to resume their normal growth and become dominated by cells with single nuclei. Thus, induction of multinuclei by ChK also did not permanently and detrimentally alter the normal epithelial WB-*neo*3 cells.

In addition to inhibition of anchorage-dependent cell growth, ChK significantly inhibited anchorage-dependent growth of WB- *ras*1 cells on soft agar. Since anchorage-dependent growth is one key feature of most tumor cells, these results demonstrate an important tumor-specific inhibitory effect of ChK on cell growth.

In order to further characterize cellular changes that accompany the inhibition of cell growth by ChK, we monitored gap junction-mediated communication, which is down-regulated in most tumor cells. A variety of antitumor compounds up-regulate gap junctional communication in tumor cells as they inhibit cell growth. Our results demonstrate that a single dose of ChK at 1 or 2 μM produced no significant change in gap junction-mediated communication between WB- *ras*1 cells following a 1 h, 6 h, 24 h, or 6 day treatment. Further experiments were performed to determine whether ChK altered connexin 43 levels in WB- *ras*1 cells, since previous studies demonstrated an ability of ChK to alter connexin 43 levels in tumor promoter-treated glial cell cultures [18] and since phosphorylation of connexin subunits has been demonstrated to contribute to gap junctional communication between cells [28].

Western blot analysis in the present studies demonstrated that vehicle-treated WB- *ras*1 cells primarily expressed the P_0 band with little P_1 and little or no P_2, as previously reported [24]. The intrinsic expression of the P_1 band varies between cultures of WB- *ras*1 cells and may increase slightly with increasing passage number. Treatment with ChK for 1, 6 h and 6 days at 1 and 2 μM, did not significantly alter the degree of connexin 43 phosphorylation in WB- *ras*1 cells. These results are in agreement with the fluorescent dye-transfer assays of gap junction-mediated communication which showed no effect of ChK at similar time points. In contrast, some compounds which inhibit growth of *ras*-transformed cells, such as PBA [26] and CAPE [25] up-regulate gap junction-mediated cellular communication with a concomitant increase in connexin 43 phosphorylation. This suggests that ChK targets different cellular pathway(s) than these other anti-Ras compounds.

ChK failed to induce a change in the total amount of p21 Ras or in the relative proportion of membrane versus cytosolic p21 Ras at 4–72 h or 5 day treatment times. This suggests that ChK does not act as an inhibitor of Ras farnesylation, in contrast to lovastatin (Fig. 6) [23].

We also tested whether MAPK or PI-3 kinase signaling pathways might be a target of ChK. No effect of ChK on p44/42 MAPK phosphorylation, a key indicator of activation, was detected (Fig. 7b). Unless ChK targets an effector downstream of p44/42 MAPK, such as Elk-1, these results suggest that ChK does not target this MAPK signaling pathway in WB- *ras*1 cells. Thus, we hypothesize that another Ras effector signaling pathway, such as the PI-3 kinase/Akt pathway, is the

target of ChK. Tikoo et al. [11] proposed that ChK may work through the Akt pathway, based on its effects on Akt phosphorylation using an in vitro phosphorylation assay. Our present results showing inhibition of Akt phosphorylation using both ser473- and thr308-specific phospho-Akt antibodies provide further evidence that the PI-3 kinase/Akt pathway is a likely target of ChK. Since Akt phosphorylation at these two sites is an indicator of activation of this cellular survival pathway [29–33], inhibition by ChK is consistent with its antitumor effects by reducing survival. Reduced phosphorylation by ChK of the Akt effector, GSK-3β [32], in WB- *ras*1 cells (Fig. 7e) provides additional evidence that ChK targets the PI-3 kinase/Akt signaling pathway.

In contrast to WB- *ras*1 cells, treatment of the untransformed WB- *neo*3 cells with ChK had no detectable effect on phosphorylation of Akt on serine 473 (Fig. 7d). This could be the basis for the reduced degree of growth

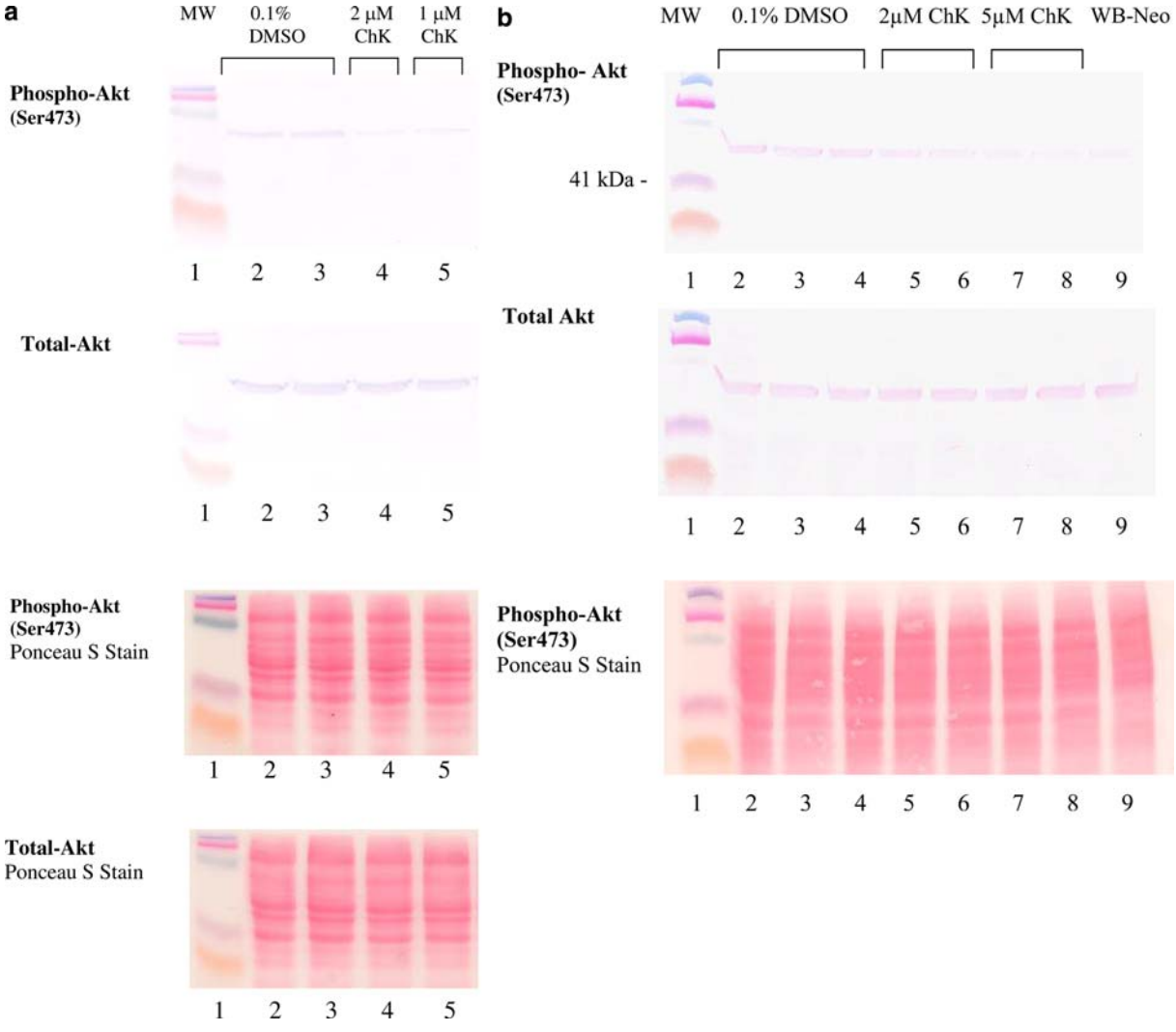

Fig. 7 Effect of ChK on Akt kinase phosphorylation. WB- *ras*1 cells were grown in 25 cm^2 flasks to 90–95% confluency, treated with vehicle or 1, 2, or 5 μM ChK, and proteins extracted for Western blot analysis using antibodies specific for total Akt or phospho-Akt. **a** Phospho-Akt(serine 473) (*top panel*) from WB- *ras*1 cells treated for 24 h with 1 or 2 μM ChK (*lanes 4 and 5*, or with vehicle (*lanes 2 and 3*). *Lane 1* shows molecular weight markers. Bottom panel shows corresponding total Akt from aliquots of the same samples loaded on a separate gel. **b** Phospho-Akt (ser473) (*top panel*) from WB- *ras*1 cells treated for 4 h with 2 or 5 μM ChK (*lanes 5–8*) or with vehicle (*lanes 2–4*, triplicates). *Lane 9* shows phospho-Akt level in untreated WB- *neo*3 cells. Lane 1 shows molecular weight markers. *Center panel* shows corresponding total Akt from aliquots of the same samples loaded on a separate gel. *Bottom panel* shows Ponceau S staining of the phospho-Akt blot before blocking with block buffer (non-fat dry milk). **c** Phospho-Akt (ser 473) (*top panel*) from WB- *neo*3 cells treated for 4 h with 5 μM ChK (*lanes 4 and 5*), with vehicle (*lanes 2 and 3*), for 24 h with 5 μM ChK (*lane 8*), or with vehicle (*lanes 6 and 7*). *Lane 1* shows molecular weight markers (Blot developed longer than **b**, *top panel*). *Bottom panel* shows corresponding total Akt from aliquots of the same samples loaded on a separate gel. **d** Phospho-Akt (thr308) (*top panel*) from WB- *ras*1 cells treated for 48 h with 1 or 2 μM ChK (*lanes 4–7*) or with vehicle (*lanes 2 and 3*). *Lane 1* shows molecular weight markers. *Center panel* shows corresponding total Akt from aliquots of the same samples loaded on a separate gel. *Bottom panel* shows Ponceau S staining of the phospho-Akt blot before blocking with block buffer (*non-fat dry milk*). **e** Phospho-GSK-3β (*top panel*) from WB- *ras*1 cells treated for 48 h with 2 μM ChK (*lanes 4 and 5*), or with vehicle (*lanes 2 and 3*). *Bottom panel* shows Ponceau S staining of the phospho-GSK-3β blot before blocking

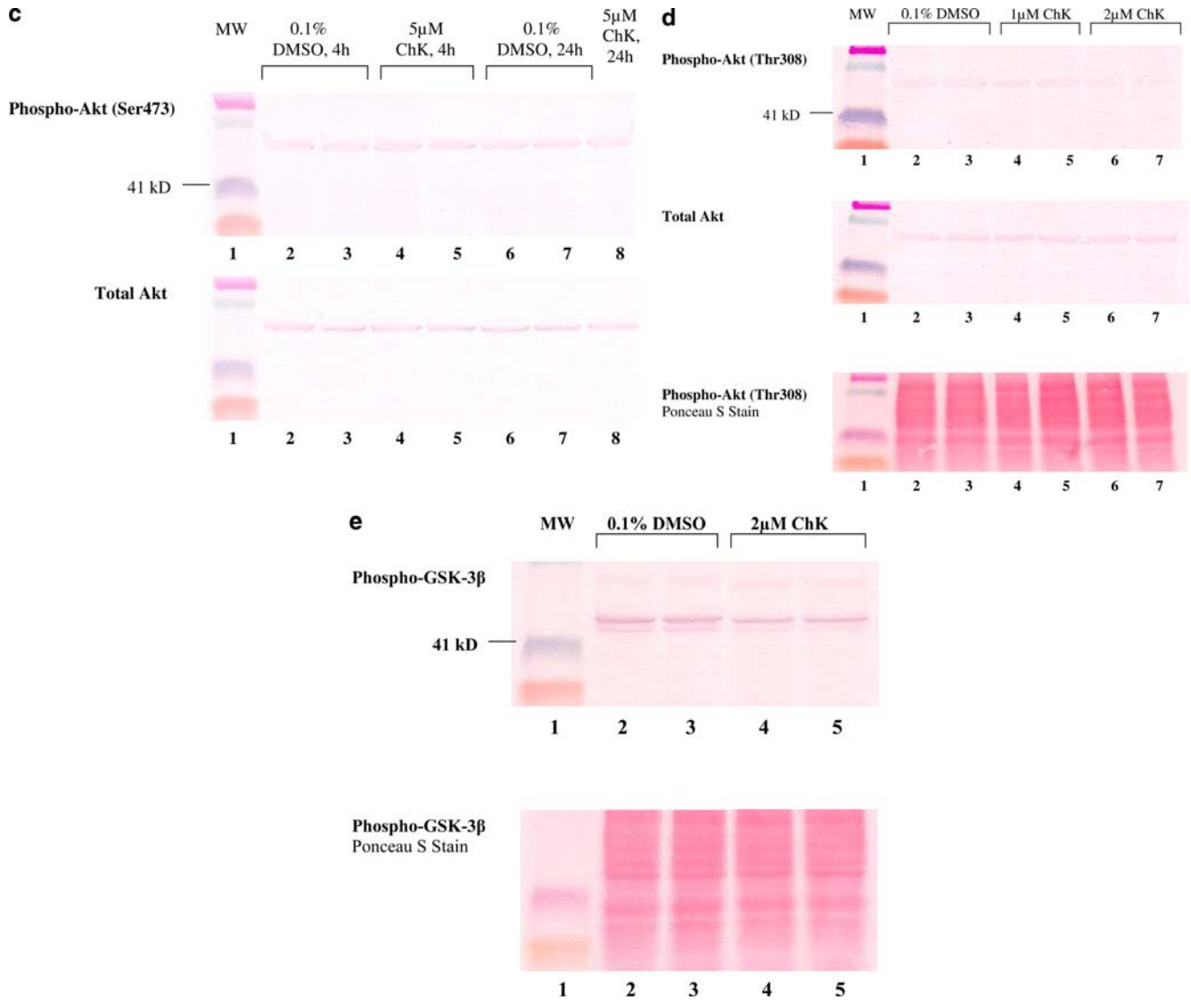

Fig. 7 (Contd.)

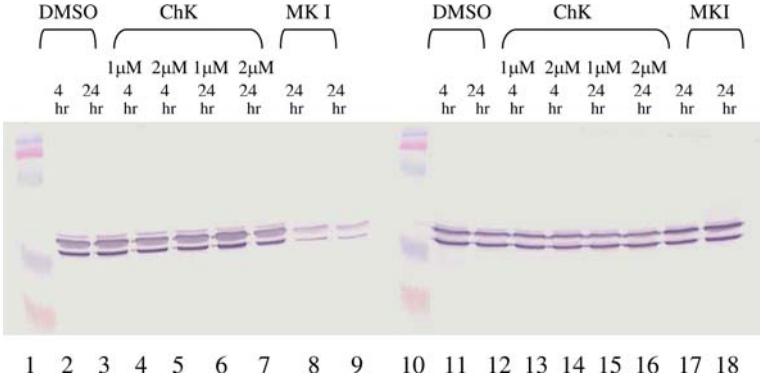

Fig. 8 Effect of ChK on p44/42 MAPK phosphorylation. WB- *ras*1 cells were grown in 25 cm^2 flasks to 90–95% confluency, treated with vehicle or 1 or 2 μM ChK for varying times as indicated and proteins extracted for Western blot analysis of phosphorylated p44/42 MAPK (lanes 1–9), or total p44/42 MAPK (lanes10–18) as described in ''Methods.'' Treatment groups were: vehicle (0.1% DMSO) for 4 h (*lane 2*) or 24 h (*lane 3*); 1 or 2 μM ChK for 4 h (*lanes 4 and 5*) or 24 h (*lanes 6 and 7*); MAPK phosphorylation inhibitor (50 μM) for 24 h (*lanes 8 and 9*, duplicates). Samples shown in lanes 10–18 were aliquots of the same samples run on a separate gel from lanes 1–9. Lanes 1 and 10 show molecular mass standards

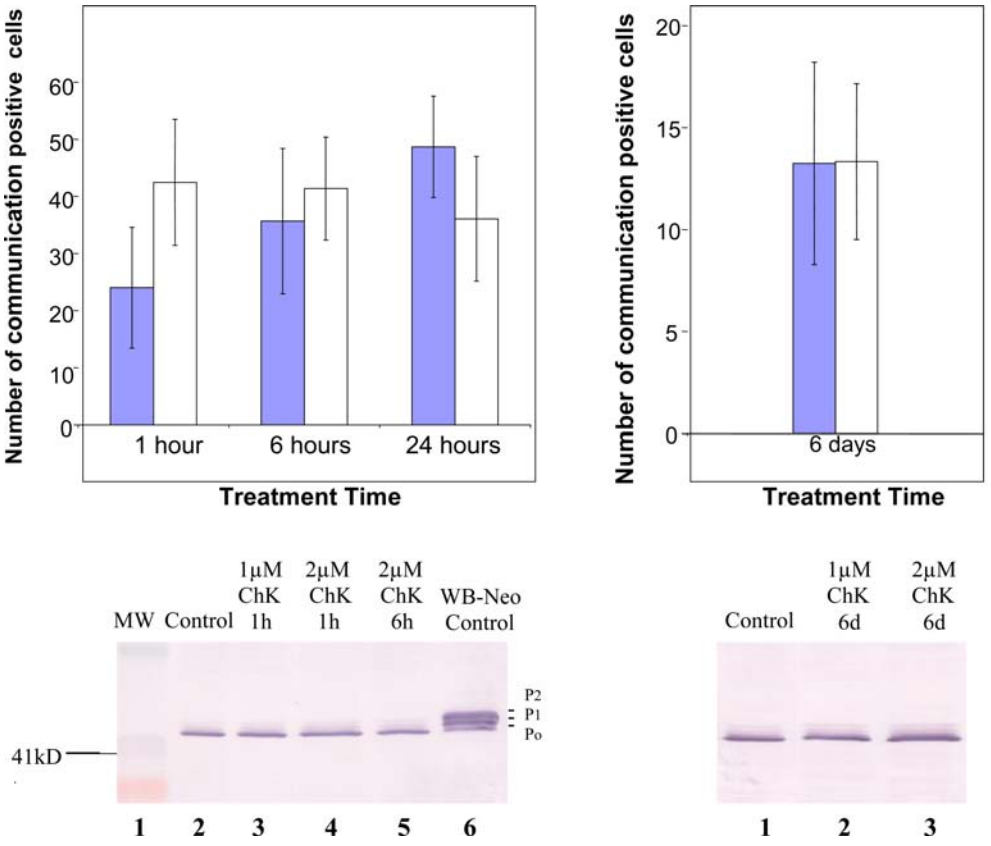

Fig. 9 Effect of ChK on fluorescent dye transfer and connexin 43 phosphorylation. For fluorescent dye transfer assays of gap junction-mediated communication (*top panels, graphs*), WB- *ras*1 cells were grown on 35 mm^2 culture dishes to 90–100% confluency and treated with 1 μM ChK for 1 h, 6 h, 24 h, or 6 days (*solid bars*). Control dishes were treated with an equal volume of DMSO (*open bars*). Data are presented as the mean ± S.D. for each group ($n = 8$ quantified areas). At least three independent experiments were performed at each treatment time. For Western blot analyses of connexin 43 phosphorylation (*lower panels*), WB- *Ras*1 cells were grown in 75 cm^2 flasks to 90–100% confluency and treated with 1 or 2 μM ChK for 1 h (*lower left panel, lanes 3 and 4*) or 6 h (*lane 5*). For 6 day treatments WB-*ras*1 cells were plated at 10–15% confluency and treated for 6 days with 1 or 2 μM ChK (*lanes 2 and 3, lower right panel*). The 41 kD molecular weight marker is shown in *lane 1* of the lower left panel. Lane 6 shows untreated WB- *neo*3 cells containing the unphosphorylated P_0, and phosphorylated P_1 and P_2 connexin 43 bands. These results are representative of triplicate independent experiments. Visualization of bands was performed as described in "Methods"

inhibition by 1 μM ChK at 6 days in WB-neo3 cells (Fig. 1b), compared to the degree of growth inhibition measured in WB-*ras*1 cells (Fig. 1a), and may reflect a less dominant Akt pathway in growth regulation of these untransformed cells.

Malik et al. [34] demonstrated that phosphorylation of Akt on serine 473 is increased in poorly differentiated prostate cancer cells. They further showed that phosphorylation on this residue is also a good predictor of poor clinical outcome in cancer patients [35]. Thus, agents such as ChK that decrease serine 473 Akt phosphorylation are prime candidates for targeted tumor therapy for these cancers.

Ras has been shown to activate PI-3 kinase directly, which leads to the activation of the Rho family protein, Rac [7]. Rac then activates enzymes that produce PIP-2, which can inactivate plus-end F actin-capping proteins such as tensin and gelsolin, leading to uncapping and polymerization of actin [32, 36]. Promotion of F-actin capping by ChK, demonstrated by Yahara et al. [37], would be expected to prevent Ras-induced actin polymerization, and therefore inhibition of cytokinesis, which is consistent with our observations.

In summary, a non-cytotoxic concentration of ChK produced antitumor effects in WB- *ras*1 cells including the inhibition of cell growth, cytokinesis, and the PI-3 kinase/Akt survival pathway. The experiments presented herein suggest that further evaluation of ChK in vitro and in vivo should be conducted to fully determine its therapeutic potential.

References

1. Adjei AA (2001) Blocking oncogenic Ras signaling for cancer therapy. J Natl Cancer Inst 93:1062–1074
2. Ahmadian MR (2002) Prospects for anti-ras drugs. Br J Haematol 116:511–518
3. Malumbres M, Barbacid M (2003) RAS oncogenes: the first 30 years. Nat Rev Cancer 3:7–13
4. Hamad NM, Elconin JH, Karnoub AE, Bai W, Rich JN, Abraham RT, Der CJ, Counter CM (2002) Distinct requirements for Ras oncogenesis in human versus mouse cells. Genes Dev 16:2045–2057

5. Cesen-Cummings K, Warner KA, Ruch RJ (1998) Role of protein kinase C in the deficient gap junctional intercellular communication of K-ras-transformed murine lung epithelial cells. Anticancer Res 18:4343–4346
6. Kolch W (2000) Meaningful relationships: the regulation of the Ras/Raf/MEK/ERK pathway by protein interactions. Biochem J 351:289–305
7. Rodriguez-Viciana P, Warne PH, Khwaja A, Marte BM, Pappin D, Das P, Waterfield MD, Ridley A, Downward J (1997) Role of phosphoinositide 3-OH kinase in cell transformation and control of the actin cytoskeleton by Ras. Cell 89:457–467
8. Urano, T, Emkey R, Feig LA (1996) Ral-GTPases mediate a distinct downstream signaling pathway from Ras that facilitates cellular transformation. EMBO J 15:810–816
9. el-Fouly MH, Trosko JE, Chang CC, Warren ST (1989) Potential role of the human Ha-ras oncogene in the inhibition of gap junctional intercellular communication. Mol Carcinog 2:131–135
10. de Feijter AW, Ray JS, Weghorst CM, Klaunig JE, Goodman JI, Chang CC, Ruch RJ, Trosko JE (1990) Infection of rat liver epithelial cells with v-Ha-ras: correlation between oncogene expression, gap junctional communication, and tumorigenicity. Mol Carcinog 3:54–67
11. Tikoo A, Cutler H, Lo SH, Chen LB, Maruta H (1999) Treatment of Ras-induced cancers by the F-actin cappers Tensin and Chaetoglobosin K, in combination with the Caspase-1 inhibitor N1445. Cancer J Sci Am 5:293–300
12. Hancock JF, Magee AI, Childs JE, Marshall CJ (1989) All *ras* proteins are polyisoprenylated but only some are palmitoylated. Cell 57:1167–1177
13. Kato K, Cox AD, Hisaka MM, Graham SM, Buss JE, Der CJ (1992) Isoprenoid addition to Ras protein is the critical modification for its membrane association and transforming activity. Proc Natl Acad Sci USA 89:6403–6407
14. Ruch RJ, Sigler K (1994) Growth inhibition of rat liver epithelial tumor cells by monoterpenes does not involve ras plasma membrane association. Carcinogenesis 15:787–789
15. Haklai R, Weisz MG, Elad G, Paz A, Marciano D, Egozi Y, Ben-Baruch G, Kloog Y (1998) Dislodgment and accelerated degredation of Ras. Biochem 37:1306–1314
16. Reuveni H, Klein S, Levitzki A (2003) The inhibition of Ras farnesylation leads to an increase in $p27^{Kip1}$ and G1 cell cycle arrest. Eur J Biochem 270:2759–2772
17. Cutler HG, Crumley F, Cox R (1980) Chaetoglobosin K: a new plant growth inhibitor and toxin from *Diplodia macrospora*. J Agric Food Chem 28:139–142
18. Matesic DF, Blommel ML, Sunman JA, Cutler SJ, Cutler HG (2001) Prevention of organochlorine-induced inhibition of gap junctional communication by chaetoglobosin K in astrocytes. Cell Biol Toxicol 17:395–408
19. Schanne FA, Kane AB, Young EE, Farber JL (1979) Calcium dependence of toxic cell death: a final common pathway. Science 206:700–702
20. Matesic DF, Rupp HL, Bonney WJ, Ruch RJ, Trosko JE (1994) Changes in gap-junction permeability, phosphorylation, and number mediated by phorbol ester and non-phorbol-ester tumor promoters in rat liver epithelial cells. Mol Carcinog 10:226–236
21. Laemmli NK (1970) Cleavage of structural proteins during the assembly of the head of bacteriophage T4. Nature 227:680–685
22. Goldman F, Hohl RJ, Crabtree J, Lewis-Tibesar K, Koretzky G (1996) Lovastatin inhibits T-cell antigen receptor signaling independent of its effects on ras. Blood 88:4611–4619
23. Ruch RJ, Madhukar BV, Trosko JE, Klaunig JE (1993) Reversal of ras-induced inhibition of gap-junctional intercellular communication, transformation, and tumorigenesis by lovastatin. Mol Carcinog 7:50–59
24. de Feijter AW, Matesic DF, Ruch RJ, Guan X, Chang CC, Trosko JE (1996) Localization and function of the connexin 43 gap-junction protein in normal and various oncogene-expressing rat liver epithelial cells. Mol Carcinog 16:203–212
25. Na HK, Wilson MR, Kang KS, Chang CC, Grunberger D, Trosko JE (2000) Restoration of gap junctional intercellular communication by caffeic acid phenethyl ester (CAPE) in a ras-transformed rat liver epithelial cell line. Cancer Lett 157:31–38
26. Sunman JA, Foster MS, Folse SL, May SW, Matesic DF (2004) Reversal of the transformed phenotype and inhibition of peptidylglycine alpha-monooxygenase in Ras-transformed cells by 4-phenyl-3-butenoic acid. Mol Carcinog 41:231–246
27. Na HK, Chang CC, Trosko JE (2003) Growth suppression of a tumorigenic rat liver cell line by the anticancer agent, ET-18-O-CH(3), is mediated by inhibition of cytokinesis. Cancer Chemother Pharmacol 51:209–215
28. Musil LS, Goodenough DA (1991) Biochemical analysis of connexin43 intracellular transport, phosphorylation, and assembly into gap-junctional plaques. J Cell Biol 115:1357–1374
29. Cross DA, Alessi DR, Cohen P, Andjelkovic M, Hemmings BA (1995) Inhibition of glycogen synthase kinase-3 by insulin mediated by protein kinase B. Nature 378:785–788
30. Alessi DR, Andjelkovic M, Caudwell B, Cron P, Morrice N, Cohen P, Hemmings BA (1996) Mechanism of activation of protein kinase B by insulin and IGF-1. EMBO J 15:6541–6551
31. Maira SM, Galetic I, Brazil DP, Kaech S, Ingley E, Thelen M, Hemmings BA (2001) Carboxyl-terminal modulator protein (CTMP), a negative regulator of PKB/Akt and v-Akt at the plasma membrane. Science 294:374–379
32. Vivanco I, Sawyers CI (2002) The phosphatidylinositol 3-kinase-Akt pathway in human cancer. Nature Rev 2:489–501
33. Stephens L, Anderson K, Stokoe D, Erdjument-Bromage H, Painter GF, Holmes AB, Gaffney PRJ, Reese CB, McCormick F, Tempst P, Coadwell J, Hawkins PT (1998) Protein kinase B kinases that mediate phosphatidylinositol 3,4,5-triphosphate-dependent activation of protein kinase B. Science 279:710–714
34. Malik SN, Brattain M, Ghosh PM, Troyer DA, Prihoda T, Bedolla R, Kreisberg JI (2002) Immunohistochemical demonstration of phospho-Akt in high Gleason grade prostate cancer. Clin Cancer Res 8:1168–1171
35. Kreisberg JI, Malik SN, Prihoda TJ, Bedolla RG, Troyer DA, Kreisberg S, Ghosh PM (2004) Phosphorylation of Akt (Ser473) is an excellent predictor of poor clinical outcome in prostate cancer. Cancer Res 64:5232–5236
36. Hartwig, JH, Bokoch GM, Carpenter CL, Janmey PA, Taylor LA, Toker A, Stossel TP (1995) Thrombin receptor ligation and activated Rac uncap actin filament barbed ends through phosphoinositide synthesis in permeabilized human platelets. Cell 82:643–653
37. Yahara I, Harada F, Sekita S, Natori S, Yoshihira K (1982) Correlation between effects of 24 different cytochalasins on cellular structures and cellular events and those on actin in vitro. J Cell Biol 92:69–87